

Inverse hormesis of cancer growth mediated by narrow ranges of tumor-directed antibodies

Oliver M. T. Pearce^{a,1}, Heinz Läubli^{a,1}, Andrea Verhagen^a, Patrick Secret^a, Jiquan Zhang^b, Nissi M. Varki^a, Paul R. Crocker^b, Jack D. Bui^c, and Ajit Varki^{a,2}

^aDepartments of Medicine and Cellular and Molecular Medicine, Glycobiology Research and Training Center, and ^cDepartment of Pathology, University of California, San Diego, La Jolla, CA 92093; and ^bCollege of Life Sciences, University of Dundee, Dundee DD1 5EH, United Kingdom

Edited by Robert A. Weinberg, Whitehead Institute for Biomedical Research, Department of Biology, Massachusetts Institute of Technology, and Ludwig/Massachusetts Institute of Technology Center for Molecular Oncology, Cambridge, MA, and approved March 5, 2014 (received for review May 29, 2012)

Compelling evidence for naturally occurring immunosurveillance against malignancies informs and justifies some current approaches toward cancer immunotherapy. However, some types of immune reactions have also been shown to facilitate tumor progression. For example, our previous studies showed that although experimental tumor growth is enhanced by low levels of circulating antibodies directed against the nonhuman sialic acid *N*-glycolylneuraminic acid (Neu5Gc), which accumulates in human tumors, growth could be inhibited by anti-Neu5Gc antibodies from a different source, in a different model. However, it remains generally unclear whether the immune responses that mediate cancer immunosurveillance vs. those responsible for inflammatory facilitation are qualitatively and/or quantitatively distinct. Here, we address this question using multiple murine tumor growth models in which polyclonal antibodies against tumor antigens, such as Neu5Gc, can alter tumor progression. We found that although growth was stimulated at low antibody doses, it was inhibited by high doses, over a linear and remarkably narrow range, defining an immune response curve (IRC; i.e., inverse hormesis). Moreover, modulation of immune responses against the tumor by altering antibody avidity or by enhancing innate immunity shifted the IRC in the appropriate direction. Thus, the dualistic role of immunosurveillance vs. inflammation in modulating tumor progression can be quantitatively distinguished in multiple model systems, and can occur over a remarkably narrow range. Similar findings were made in a human tumor xenograft model using a narrow range of doses of a monoclonal antibody currently in clinical use. These findings may have implications for the etiology, prevention, and treatment of cancer.

tumor-associated macrophages | M2 polarization | NK cells | antibody-dependent cellular cytotoxicity

The concept that host immunity might eliminate cancer cells is over 100 y old (1). In the 1950s, Burnet (2) noted that nascent transformed cells must occur at high frequency in long-lived mammals, and therefore proposed a process of “immunosurveillance” in which the immune system is constantly checking for and neutralizing intrinsic cells with transformed phenotypes. Much progress has been made since then in understanding the role of the immune system in both tumorigenesis and tumor progression. In particular, the host-protective and tumor-sculpting activity of the immune system has been proposed in a process termed cancer “immunoediting” (3, 4), consisting of three distinct steps: elimination, in which the immune system is constantly deleting mutated cells; equilibrium, during which cancer cell division is kept in check by immune-mediated destruction; and escape, wherein the genetically selected and evolved tumor cell overcomes immune suppression and expands uncontrollably.

In contrast, another large body of literature indicates that immune reactions induced by different mechanisms, such as chronic inflammation from infectious or noninfectious agents, can paradoxically support and stimulate the growth of cancers

(5–10). In these studies, chronic inflammation is shown to promote tumor formation via activation of inflammatory pathways, such as the NF- κ B pathway and STAT3, which can induce cytokine production in immune cells, further supporting tumor progression (10, 11). In keeping with this finding, anti-inflammatory agents, such as aspirin, can reduce cancer risk (12). It is uncertain whether the inflammatory responses during cancer formation and cancer progression are directly associated with immunosurveillance or can be seen as separate, overlapping processes (13). Nevertheless, it is clear that the immune system plays a dualistic role in the progression of tumors depending on the exact context and tumor stage at which the interaction with malignant cells takes place. This explains studies in which an immune reactant inhibits tumor formation and/or growth, whereas the very same reactant has a tumor-promoting effect in another model (14). Other inflammatory effectors that play paradoxical roles in mammalian tumor proliferation include NF- κ B (15), MyD88 (16, 17), IL-1 β (18), and IFN- γ (19). The immune effectors (“reactants”) involved can range from antibodies (20–23) to tumor-associated macrophages (TAMs) (24–26), contributing to an altered microenvironment that favors tumor progression (26, 27). Inflammatory aspects of cancer and the

Significance

We have previously shown that antibodies directed against tumor-associated antigens containing the nonhuman sialic acid *N*-glycolylneuraminic acid (Neu5Gc) can influence tumor progression. Here, we analyzed growth of Neu5Gc-positive tumors in Neu5Gc-deficient mice, following administration of increasing concentrations of anti-Neu5Gc antibodies. Although lower antibody concentrations stimulated tumor growth, higher concentrations inhibited growth, over a surprisingly narrow dose range. This biphasic narrow-range tumor growth response to tumor-directed antibodies (inverse hormesis) was reproduced in multiple mouse models, including one using a clinically approved monoclonal antibody. Our results are a novel experimental demonstration of how the levels of circulating antibodies can differentially influence tumor growth. These findings might have important implications in natural cancer progression and/or in cancer immunotherapy with antibodies.

Author contributions: O.M.T.P., H.L., J.D.B., and A. Varki designed research; O.M.T.P., H.L., A. Verhagen, and P.S. performed research; J.Z., N.M.V., and P.R.C. contributed new reagents/analytic tools; O.M.T.P. and H.L. analyzed data; and O.M.T.P., H.L., J.D.B., and A. Varki wrote the paper.

Conflict of interest statement: A. Varki and N.M.V. are cofounders of and advisors to Sialix, Inc., which has licensed University of California, San Diego technologies related to anti-Neu5Gc antibodies in cancer.

This article is a PNAS Direct Submission.

¹O.M.T.P. and H.L. contributed equally to this work.

²To whom correspondence should be addressed. E-mail: a1varki@ucsd.edu.

This article contains supporting information online at www.pnas.org/lookup/suppl/doi:10.1073/pnas.1209067111/-DCSupplemental.

need for tumors to escape immune surveillance have recently been noted as emerging “hallmarks of cancer” (28).

We have previously shown that low concentrations of murine polyclonal antibodies against tumor antigens with glycans expressing the sialic acid *N*-glycolyl-neuraminic acid (Neu5Gc) can promote tumor growth via a COX-2 dependent mechanism involving myeloid cells, such as TAMs (29). In another model and with a different source of antibodies, polyclonal anti-Neu5Gc antibodies were able to inhibit tumor growth via increasing antibody-dependent cellular cytotoxicity (ADCC) and complement-dependent cytotoxicity mechanisms (30). Because the same immune reactants can potentially promote or suppress tumor growth, we wondered if it is possible that the quantity of immune reactants determines the effect on tumor growth, as proposed by Prehn (31) in the 1970s. In Prehn’s early studies (31), low doses of splenocytes directed against a growing tumor could stimulate tumor growth in a dose-dependent fashion. In other work, Andrews (32) showed that putting chemically induced papillomas into an immune-depressed murine background led to regression of the tumor rather than expansion. These and other data led to the proposal of a hypothetical immune response curve (IRC) (Fig. 1*A*), updated by Prehn (33), in which the response of the tumor would be dependent on the quantity and quality of the immune reaction. However, this hypothesis has not been modeled experimentally in a single system, and the range over which such an IRC might occur has not been defined.

We asked what effect a range of tumor-directed antibody doses has on tumor progression, using our previously well-characterized murine polyclonal tumor antibody model involving the tumor antigen Neu5Gc (29). We found that there was indeed a link between dose and tumor proliferation and inhibition as predicted by Prehn (31, 33). Surprisingly, the antibody dose range over which these dualistic effects occurred was found to be remarkably narrow. Furthermore, the resulting IRC could be shifted by altering the quality of the antibody or by increasing innate immunity (as a model of additive effects). We also replicate the narrow-range IRC in other cancer models involving polyclonal or monoclonal antibodies, suggesting this phenomenon could be

a general effect, and analyze the cellular mechanisms involved, implicating infiltrating TAMs and natural killer (NK) cells in our model systems.

Results

Dualistic Response of Tumor Growth to Tumor-Specific Anti-Neu5Gc IgG in Human-Like Neu5Gc-Deficient Mice. To assess a tumor IRC experimentally in a single-model system, we studied our previously established model of chronic inflammation-induced cancer progression, involving antibodies against the nonhuman glycan antigen Neu5Gc, which we have shown to accumulate in human tumors from dietary sources (34). To mimic the human condition of Neu5Gc deficiency we used Neu5Gc-deficient *Cmah* null mice bearing a syngeneic mouse MC38 colon carcinoma, a tumor line expressing surface Neu5Gc at levels comparable to those seen in human carcinoma samples (29). To ensure quantitative precision, we used preabsorbed, monospecific, and carefully controlled polyclonal antisera that were generated as previously described (29). The anti-Neu5Gc specificity of the sera (and the lack of reactivity of the control-immunized serum) was confirmed for the MC38 cell line (Fig. S1).

To model an IRC experimentally, we analyzed the growth kinetics of s.c. MC38 flank tumors following transfer of anti-Neu5Gc IgG over a dose range of 14–56 μ g. We found that a dose of 14 μ g was stimulatory for tumor size and that the effect was enhanced by doubling the dose to 28 μ g (Fig. 1*B*), an effect that we have previously reported (29). However, further doubling the dose to 56 μ g was inhibitory for tumor growth. This finding was confirmed by measurements of tumor masses at the end point (Fig. 1*C* and Fig. S2). We also confirmed the previous finding (29) that control sera (from control-immunized mice that did not generate anti-Neu5Gc antibodies) had no effect on tumor growth (Fig. S2). From this experiment, we predicted that an intermediate dose of 40 μ g should generate tumors with masses that fall somewhere between the 28- μ g and 56- μ g doses. This was indeed the case, with 40 μ g having only a small, insignificant effect on tumor growth (Fig. S2*D* and *F*). Plotting the results from multiple experiments comparing different doses in *Cmah* null mice with control mice (Fig. S2) as the percentage difference in tumor growth vs. antibody dose resulted in an IRC that fitted well with Prehn’s theoretical curve (33) (compare Fig. 1*A* and *D*). We examined the immune cell infiltrates in the tumor microenvironment (Fig. S3*A*) and found that tumors growing faster as a result of antibody stimulation were infiltrated with an increased number of F4/80⁺ TAMs compared with tumors from mice treated with control antibody. Conversely, in tumors in which growth was inhibited by antibody, we saw less infiltration of F4/80⁺ cells. We also observed areas with increased accumulation of NK cells within tumors of mice treated with an inhibiting dose (Fig. S3*B*).

Hormesis is a term describing how a drug or other effector is therapeutic at lower doses but harmful/toxic at higher doses (35). Because the effect of antibodies on tumor growth is the opposite, with higher doses actually being beneficial to the host, the observed curve is an example of “inverse hormesis.” The results allow predictions about how the quality and quantity of the immune response might influence the shape of the IRC.

Reduction in Avidity of the Antibody Shifts the IRC to the Right.

Prehn predicted that a reduction in “immune quality” would shift the IRC to the right (33). To test this prediction, we repeated the IRC with another polyclonal anti-Neu5Gc antibody preparation that displayed decreased overall binding to surface Neu5Gc on MC38 cells, as assayed by flow cytometry. As shown in Fig. 2*A*, maximal staining with this second antibody was four- to fivefold decreased compared with the first antibody, indicating a lower overall avidity of binding to Neu5Gc. The difference in overall avidity was shown to be due to different preferences for

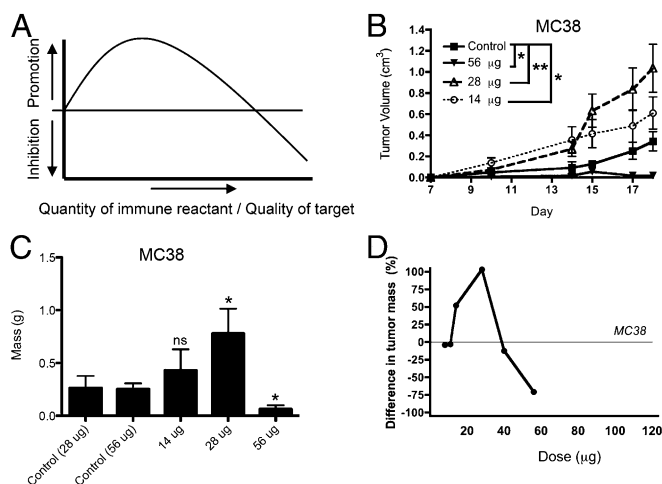


Fig. 1. Demonstration of the dualistic IRC. (A) Hypothetical IRC. (B) Example of tumor growth kinetics determined by measuring tumor volume with varying doses of antibody-containing sera ($n = 7$). (C) Tumor weights over a dose range. Sera from mice immunized against human erythrocyte ghosts ($n = 7$) were used as a control (Methods). (D) Difference in tumor growth plotted against the dose (an IRC) of the antibody (immune reaction) is an example of inverse hormesis. Statistical analysis was done using two-way ANOVA for growth curves or a *t* test for tumor weights. * $P < 0.05$; ** $P < 0.01$. ns, not significant.

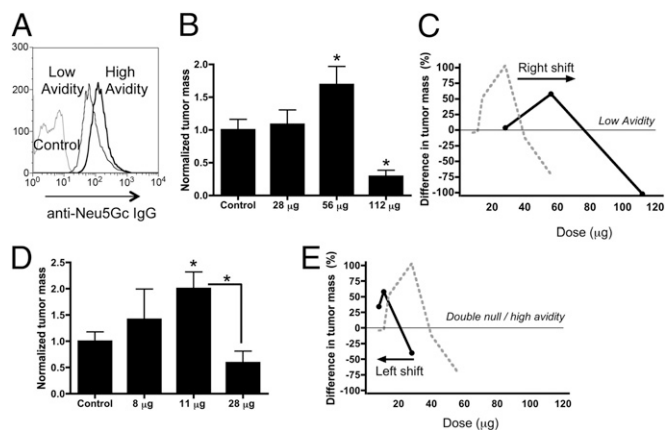


Fig. 2. Change in the quality of the immune reactant shifts the IRC to the right. (A) Flow cytometry of the MC38 cell line using anti-Neu5Gc antibodies of high avidity (as used in Fig. 1) or low avidity (as used in this figure). (B) Normalized tumor weights at the end point ($n = 7$). (C) Corresponding IRC for the effect of low-avidity sera on MC38 tumor growth. (D) Normalized tumor mass over several experiments in *Cmah*^{-/-} *SigE*^{-/-} double-deficient mice ($n = 7$ per experiment). (E) Corresponding IRC for the model containing additional immune pressure against the tumor cell line. Statistical analysis was done by a t test. * $P < 0.05$.

Neu5Gc linkages to the cell surface (Fig. S4 A and B), whereas the specificity for Neu5Gc remained unchanged. When we generated an IRC for the low-avidity sera from the tumor weights at the same end point as before (Fig. 2B), this data demonstrated a right shift of the IRC (Fig. 2C), which fits with the predicted effect of reducing the quality of the immune reactant.

Reduced Levels of Inhibitory Leukocyte Siglecs Correlate with Increased Inflammatory Response and Shift the IRC to the Left.

We next predicted that the addition of a second immune stimulating factor would shift the IRC to the left. We sought to model another human-like condition affecting the immune response by evaluating expression levels of immunomodulatory receptors called Siglecs found on cells of the immune system (36, 37). Lower levels of inhibitory Siglecs have been reported previously in human lymphocytes compared with those of chimpanzees, and have been correlated with an enhanced production of proinflammatory cytokines (38). Although human and mouse Siglecs have undergone significant evolutionary divergence, Siglec-E in the mouse is the functionally equivalent homolog of the inhibitory human Siglec-9, being expressed prominently on myeloid cells (39). The Siglec-E-deficient *Siglece*-null (*SigE*^{-/-}) mouse has recently been described (40), wherein an overreactive myelomonocytic cell phenotype was demonstrated. To investigate whether expression levels of this innate immune inhibitory Siglec modulate inflammatory responses associated with tumor progression, we compared tumor growth in *SigE*^{-/-} mice vs. littermate controlled WT mice. There was a significant delay in the initial appearance of tumors, likely due to an enhanced innate immune response generated against the MC38 tumor in the *SigE*^{-/-} mice (Fig. S4C).

To test the effects of altering multiple immune reactants on the IRC (namely, the effects of the anti-Neu5Gc antibodies, in combination with the impact of the absence of Siglec-E), we used a *Cmah*^{-/-} *SigE*^{-/-} double-deficient murine model and studied the kinetics of tumor growth as before (Fig. 2D and Fig. S4D). In this model, we were able to reproduce the inverse hormetic effect of tumor antibodies on growth, but this effect occurred over a different dose range. For example, a dose of 11 μ g (which had no effect on tumor growth in the presence of Siglec-E; Fig. 1D) stimulated tumor growth, whereas a dose of 28 μ g (which

was stimulating in the presence of Siglec-E; Fig. 1D) now inhibited growth (Fig. 2D). When we analyzed the tumor weights at the end point, the 28- μ g dose was not statistically significant. However, the effect was confirmed as biphasic when comparing the 11- μ g dose with the 28- μ g dose (Fig. 2D). Additionally, the delay in tumor growth seen in the absence of Siglec-E (Fig. S4D) was enhanced in the presence of the 28- μ g antibody dose (Fig. S4E), further supporting an inhibitory effect. Overall, these data show a left shift in the IRC, presumably as a result of an additive effect of increased inflammatory background from enhanced myeloid activation on which a lower dose of antibody is required to achieve the same stimulation and inhibition effect (Fig. 2E).

Reproduction of the IRC Using Polyclonal Tumor Antisera.

In the above studies, growth of MC38 tumors in the absence of antibody might also be partially affected by adaptive immunity (i.e., despite being syngeneic, it has some intrinsic immunogenicity). Indeed, we found slower growth in WT syngeneic mice vs. *Rag1*^{-/-} mice, which lack adaptive immunity (Fig. 3A). To test if inverse hormesis could be seen with another polyclonal antibody model in an immunocompetent host, we took advantage of the spontaneous generation of antibodies against s.c. MC38 tumors. We reasoned that because the MC38 tumor undergoes delayed growth in a WT mouse (Fig. 3A), it could be that mice will generate antibodies against the tumor. To test this possibility, we analyzed sera from WT mice that had been previously challenged with MC38 tumors for at least 15 d. We isolated two pools of sera, one that showed strong IgG binding to MC38 cells (Fig. 3B; high) and one that showed weak IgG binding to MC38 cells (Fig. 3B; low, but it is unclear whether this observation is a result of lower avidity or just lower antibody titers). Sera from WT mice that had not been challenged with MC38 tumors showed no natural/nonspecific IgG binding against the MC38 cells (Fig. 3B). As before, we examined the effect of antiserum dose on subcutaneous tumor growth of both high- and low-level sera in WT mice inoculated with MC38 cells. Using a “high-level” serum concentration of 1:4–1:2, tumor stimulation was observed, and at a 1:1 dose of sera, the stimulation effect disappeared (Fig. 3C).

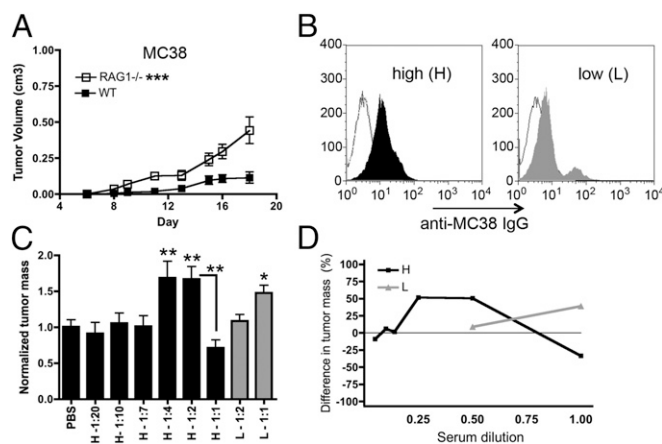


Fig. 3. Hormesis of tumor progression using a second antitumor IgG antibody derived from C57BL/6 mice exposed to the MC38 tumor. (A) Growth kinetics of MC38 tumor cell line compared between the *Rag1*-deficient mouse model and the C57BL/6 WT model ($n = 5$). (B) Flow cytometry of sera isolated from mice 15 d after inoculation with MC38 cells (compared to control sera from a naive WT mouse). (C) Normalized tumor weights taken over multiple experiments. Tumors were isolated 18 d after inoculation. Dose is given as a dilution in PBS. (D) IRC of tumor response generated from C. Tumor weights were analyzed by a t test. * $P < 0.05$; ** $P < 0.005$; *** $P < 0.001$. H, high-level sera; L, low-level sera.

Thus, the observed effect was bimodal, similar to the observed response to anti-Neu5Gc polyclonal antibodies. Accordingly, at the same concentration, “low-level” sera did not stimulate tumor growth. Only at a 1:1 dose was stimulation seen (Fig. 3 C and D, gray bars/line), which was predictable from the observed level of staining seen by flow cytometry (Fig. 3B). Along with Fig. 3C and the control sera used throughout, this finding further supports the notion that stimulation or inhibition is a direct result of the antibody interaction within the tumor microenvironment and not the result of some other factor within the serum.

Reproduction of the IRC Using a Different Tumor Cell Line That Is Already Edited. So far, all studies used a single-tumor line that had not yet been completely edited (i.e., it generates an antibody response). To test whether the IRC could be seen in tumors that have fully “escaped” (3) immune editing and are poorly immunogenic, we used a Lewis lung carcinoma (LLC) cell line, which has a similar level of Neu5Gc expression on the surface as MC38 cells (Fig. S5) and similar growth kinetics between the *Rag1*^{-/-} and C57BL/6 WT mice (Fig. 4A). As before, a hormetic effect was seen with the anti-Neu5Gc sera, confirmed by the growth kinetics and the tumor masses at the end point (Fig. 4B and C), which allowed another narrow-range IRC to be drawn (Fig. 4D).

IRC Analysis with a Clinically Relevant Monoclonal Antibody in Athymic Mice. In the syngeneic model, we noted an increase in F4/80⁺ TAMs after applying stimulating doses and a decrease with the tumor-inhibiting doses (Fig. S3A). Moreover, we found areas with infiltration of NK cells in s.c. tumors when we used the tumor-inhibiting dose (Fig. S3B). This led us to suspect that hormesis could occur independent of the adaptive immune system. To test if the observed IRC is largely independent of T cells, we used another mouse model, athymic nude mice in a BALB/c background. In addition, we took this opportunity to study a clinically relevant monoclonal antibody. We used the human CD20-positive Burkitt lymphoma cell line Ramos (Fig. S6A) with the clinically widely used anti-CD20 monoclonal antibody rituximab over a range of doses. We tested hormesis with a range

of antibody from 1 to 0.1 mg/kg, because we found strong inhibition of growth in pilot experiments at doses above 1 mg/kg. We found that although doses of 0.5 mg/kg still had an inhibitory effect on tumor growth, an even lower dose of 0.1 mg/kg significantly accelerated tumor growth (Fig. 5A).

Roles of TAMs and NK Cells in the Burkitt Model. As with the syngeneic model (Fig. S3A), analysis of tumor-infiltrating leukocytes [TILs (CD45⁺)] in the tumor microenvironment revealed an increase in CD11b⁺ F4/80⁺ cell infiltration with this stimulating dose (Fig. 5B and Fig. S6B) not seen with the 0.5-mg/kg inhibitory dose. Moreover, gating on CD11b⁺ tumor-infiltrating myeloid cells (Fig. S6C) showed a clear increase in F4/80⁺ CD206⁺ M2-polarized TAMs at the 0.1-mg/kg stimulating dose and a decrease in F4/80⁺ CD206⁺ M2-polarized TAMs in the 0.5-mg/kg inhibiting dose compared with the control dose, similar to what was seen previously (Fig. 5C and Fig. S6C). It has previously been shown that the binding of the Fc region of an antibody to the Fc receptors on TAMs can stimulate tumor growth (20). To determine whether enhanced tumor growth within the hormesis model was, in part, dependent on TAMs, we next used clodronate liposomes (41) to deplete macrophages before administration of rituximab. In the absence of macrophages, tumor growth was no longer enhanced by antibody (Fig. 5D). There was even a trend to a reduced growth rate compared with an irrelevant IgG used as a control in this experiment, indicating an inhibitory function of rituximab at this low dose after treatment with clodronate liposomes. We could observe some macrophage infiltration into tumors 8 d after rituximab injection (10 d after clodronate application), but it was strongly reduced in comparison to tumors from mice with liposome treatment (Fig. S7A and B). No differences between clodronate-treated and liposome control animals were seen when using 0.5 mg/kg of rituximab or PBS as a control (Fig. S7C). Similar to the syngeneic model, an increased infiltration of NK cells was observed in Ramos tumors exposed to growth-inhibiting doses of rituximab (Fig. S8). Depletion of NK cells before administration of rituximab at an inhibiting dose led to a reversal of tumor growth inhibition (Fig. 5E) indicating that ADCC by NK cells mediates the inhibiting part of the IRC in this model.

Taken together, these data indicate that the hormetic effect can occur independent of the adaptive immune system and is dependent on interactions of the antibody with TAMs and NK cells within the tumor microenvironment. Importantly, this finding also demonstrates that hormesis can occur with monoclonal antibody preparations and provides a fourth model of the narrow-range IRC concept (summarized in Fig. 6).

Discussion

We have demonstrated here that tumor-directed antibodies can stimulate or inhibit tumor progression within single-model systems, depending on the dose. Surprisingly, this inverse hormesis can occur over a remarkably narrow and linear range of antibody levels. Also, whereas antibodies with lower avidity shifted the IRC to the right, removing the immunosuppressive Siglec-E shifted it back to the left (Fig. 2). These results fit with Prehn's predictions that not only quantity but changes in the quality of immune reactants can affect the outcome of the immune response to cancers (31, 33). We confirmed our initial observation that polyclonal antibodies within our Neu5Gc model follow an inverse hormetic curve with other models of antibodies (tumor antisera and monoclonal clinically used antibody), changing the reactivity of cells involved (*SigE*^{-/-} mice), modifying the mouse model and strain (C57BL/6, BALB/c, and immunodeficient models), and analyzing different tumor cell lines (syngeneic MC38, LLC cells, and xenogeneic human lymphoma cells). It is likely that the growth-promoting capacity of rituximab in similar models was missed in earlier studies, because doses were not

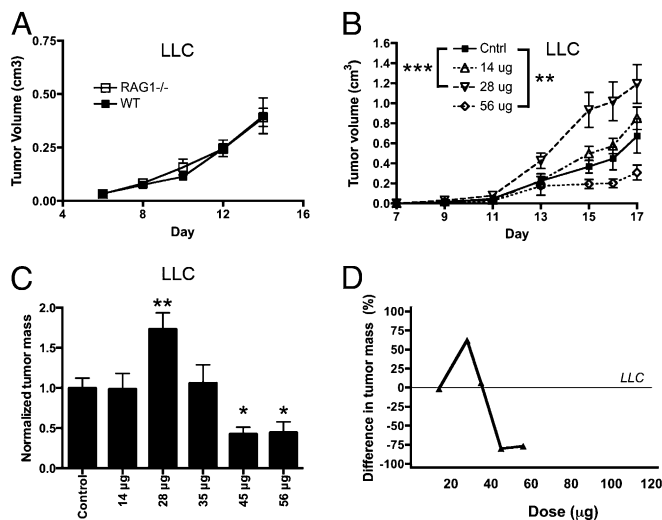


Fig. 4. Antibody-mediated inverse hormesis also occurs in a poorly immunogenic tumor cell line. (A) Growth kinetics of LLC tumor cells growing in WT or RAG1-deficient mice ($n = 5$). (B) Example of tumor growth kinetics determined by measuring tumor volume with varying doses of antibody-containing sera ($n = 7$). (C) Normalized tumor weights at the end point from two comparable experiments ($n = 7$ per experiment). (D) Corresponding IRC for the LLC tumor cell line. Statistical analysis was done using two-way ANOVA for growth curves or a t test for tumor weights. * $P < 0.05$; ** $P < 0.01$; *** $P < 0.001$.

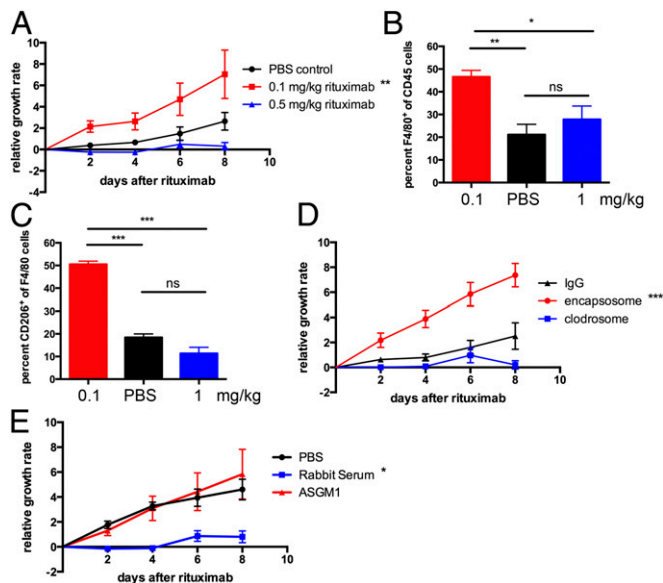


Fig. 5. Inverse hormesis also occurs in the absence of the adaptive immune system and with a therapeutic monoclonal antibody. (A) Relative growth rates of s.c. Ramos tumors in athymic nude mice after treatment with different doses of rituximab and PBS as a control ($n = 8$). (B) Analysis of CD11b⁺ F4/80⁺ tumor-infiltrating leukocytes by flow cytometry. (C) Statistical analysis of infiltrating F4/80⁺ CD206⁺ macrophage population by flow cytometry. (D) Relative growth rates of Ramos tumors after 0.1-mg/kg rituximab injection in mice depleted of macrophages with clodronate-containing liposomes (clodrosomes) compared with control liposomes (encapsosome) and irrelevant IgG ($n = 8-10$). (E) Relative growth rates of Ramos tumors after 1 mg/kg of rituximab or PBS control treatment in mice depleted of NK cells with antisialo GM1 antiserum (ASGM1) or control rabbit serum ($n = 10$). Statistical analysis was done using two-way ANOVA for growth curves or one-way ANOVA for FACS analysis. * $P < 0.05$; ** $P < 0.01$; *** $P < 0.001$.

titrated to such low ranges. We do realize that tumor isograft and xenograft models have limitations, particularly with regard to the recapitulation of the tumor microenvironment. However, these models allowed a controlled and well-timed experiment that would be very difficult to control experimentally in an autochthonous tumor model.

Although further work is necessary to determine the relevance of these findings to the clinical setting, there are potential implications for immunotherapies. For example, patients who undergo monotherapies with rituximab for low-grade CD20-positive B-cell lymphoma show progressive disease in up to 10% of cases rapidly after administration of the first dose (42). Although this observation might be due to an escape of resistant clones and other resistance mechanisms, the IRC could, in some part, explain this phenomenon as a function of the evolving inflammatory response that occurs within the tumor microenvironment during treatment.

The IRC is independent of the adaptive immune system, because athymic mice still exhibit a biphasic immune response to increasing doses of rituximab (Fig. 5) and fully edited LLC tumor cells show a similar IRC (Fig. 4). We further demonstrated by depletion experiments that M2-polarized TAMs are responsible for the tumor promoting and NK cells are responsible for the inhibitory effect seen in the rituximab model. The surprisingly narrow range between promoting and inhibitory effects could be potentially explained by simultaneously opposing forces of M2 TAM-mediated growth promotion and NK cell-mediated growth inhibition, in which lower doses favor M2 TAM expansion and higher doses promote NK cell-mediated ADCC. There is evidence that binding of antibodies to Fc γ receptors on TILs, such as macrophages, stimulates tumor growth (20). Andreu et al.

(21) found in mice that develop skin tumors due to expression of the early region of HPV16 under the promoter of K14 that the previously described promotion of tumor progression by IgG was lost if they used mice deficient for Fc γ receptors (20). They further described an Fc γ receptor-dependent polarization of F4/80⁺ CD11b⁺ TAMs to tumor-promoting M2 phenotypes (20), similar to what we observed in our athymic nude mouse model after transferring rituximab. The NK cell-dependent inhibition of tumor growth in our model is also presumably mediated by Fc γ receptors and ADCC (43). Thus, future analysis of the IRC should examine the function of inhibiting and stimulating Fc γ receptors on innate immune cells. The role of complement activation in the IRC mediated by antibodies should also be further studied.

Here, we also pursued our earlier findings that antibodies against Neu5Gc can alter tumor growth. The biology of sialic acids in humans is unusual in comparison to our closest relatives, first, in our deficiency for Neu5Gc biosynthesis and, second, with regard to reduced immunoregulatory Siglec expression on lymphocytes (38). Human carcinomas are epidemiologically associated with diets that are high in red meats (44–53), foods that are also enriched with the nonhuman antigen Neu5Gc (34). The combination of metabolically incorporated antigen (Neu5Gc) and the corresponding antibody (anti-Neu5Gc) (30), along with overreactive leukocytes, could be, in part, responsible for exacerbation of chronic inflammatory responses that occur in human epithelial linings and tumorigenesis (5, 54). Taken together, this combination of factors may contribute to the higher frequency of carcinomas in humans compared with other hominids (55, 56). Although the data presented here are from experimental model systems, there may also be naturally occurring instances in humans where the line between immune facilitation and suppression of cancer is as narrow as shown here. If so, dualistic effects may be confounding interpretation of studies of both the immunoprevention of cancer (via deliberate reduction of inflammation) and the immunotherapy of cancer (by directed immune responses). In such cases as anti-Neu5Gc antibodies interacting with Neu5Gc-containing tumors, it may be possible to manipulate the relevant components in a direction that favors a better outcome for the host.

In conclusion, we have presented evidence in multiple *in vivo* models that the quantity of an immune reactant (antibodies in this case) determines the outcome of the interaction between the immune system and malignant cells. As discussed above, this finding has potential implications for the therapy and prevention of cancer and warrants further studies to determine the exact mechanism and means to interfere with tumor-promoting effects while augmenting tumor eradication.

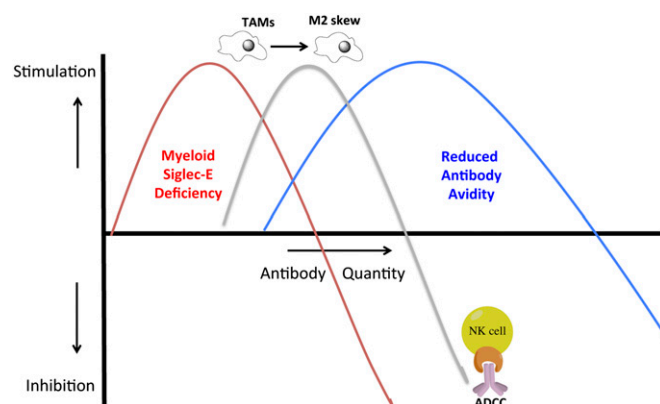


Fig. 6. Summary of findings. The quantity and quality of antibody-mediated inverse hormesis can influence tumor growth, with effects mediated by NK cells or TAMs.

Methods

Anti-Neu5Gc Antibodies and Tumor Growth Studies. Tumor cells were administered by s.c. injection to the shaved right flank of the animal. Tumors were measured using calipers in three dimensions.

Polyclonal IgG or tumor antisera were administered (i.p.) 5 d after tumor cell inoculation. All tumors were removed at day 22, or earlier if necessary. Experiments that showed a positive or negative effect of antibodies on tumor growth were repeated at least once, and multiple times in some cases. Although the final conclusion from each individual experiment was comparable, the magnitude of the effect on tumor growth could vary. Therefore, to present the data in their most representative form, normalized tumor weights are shown.

Athymic Nude Mouse Model. Ramos tumor cells were grown as described above, and 5×10^5 cells were injected s.c. into the right flank of athymic mice (BALB/c). After 14 d, depletion of macrophages with clodronate liposomes

(clodronate; Encapsula Nano Sciences) or of NK cells with antisialo GM1 (ASGM1; Wako) was performed. We injected 100 μ L of clodronate liposomes or empty control liposomes (i.v.) for macrophage depletion. Two days later, we applied different doses of rituximab (Rituxan; Genentech, Inc.) i.p., and the change in tumor volume was followed over several days. The change in tumor volumes was normalized by dividing through the average size on the day of rituximab injection and presented as the relative growth rate.

ACKNOWLEDGMENTS. We thank Christopher J. Gregg, Kalyan Banda, and Vered Padler-Karavani for advice on some of the experiments and for discussions, and Renee Chow, Andrea Garcia, and Siavesh Assar (Histology Core facility) for assistance with data collection. This work was supported by a Samuel and Ruth Engelberg Fellowship from the Cancer Research Institute (to O.M.T.P.), by the Swiss National Science Foundation (H.L.), and by Grant R01CA38701 from the National Institutes of Health to (to A. Varki).

- Ehrlich P (1909) Ueber den jetzigen stand der Karzinomforschung. *Ned Tijdschr Geneesk* 5:273. Dutch.
- Burnet M (1957) Cancer: A biological approach. III. Viruses associated with neoplastic conditions. IV. Practical applications. *BMJ* 1(5023):841–847.
- Dunn GP, Bruce AT, Ikeda H, Old LJ, Schreiber RD (2002) Cancer immunoeediting: From immunosurveillance to tumor escape. *Nat Immunol* 3(11):991–998.
- Dunn GP, Old LJ, Schreiber RD (2004) The three Es of cancer immunoeediting. *Annu Rev Immunol* 22:329–360.
- Coussens LM, Werb Z (2002) Inflammation and cancer. *Nature* 420(6917):860–867.
- Dinarello CA (2006) The paradox of pro-inflammatory cytokines in cancer. *Cancer Metastasis Rev* 25(3):307–313.
- Mantovani A, Romero P, Palucka AK, Marincola FM (2008) Tumour immunity: Effector response to tumour and role of the microenvironment. *Lancet* 371(9614):771–783.
- Mantovani A, Allavena P, Sica A, Balkwill F (2008) Cancer-related inflammation. *Nature* 454(7203):436–444.
- zur Hausen H (2009) Papillomaviruses in the causation of human cancers—A brief historical account. *Virology* 384(2):260–265.
- Grivninkov SI, Gretten FR, Karin M (2010) Immunity, inflammation, and cancer. *Cell* 140(6):883–899.
- Elinav E, et al. (2013) Inflammation-induced cancer: Crosstalk between tumours, immune cells and microorganisms. *Nat Rev Cancer* 13(11):759–771.
- Rothwell PM, et al. (2011) Effect of daily aspirin on long-term risk of death due to cancer: Analysis of individual patient data from randomised trials. *Lancet* 377(9759):31–41.
- Bui JD, Schreiber RD (2007) Cancer immunosurveillance, immunoeediting and inflammation: Independent or interdependent processes? *Curr Opin Immunol* 19(2):203–208.
- Schreiber RD, Old LJ, Smyth MJ (2011) Cancer immunoeediting: Integrating immunity's roles in cancer suppression and promotion. *Science* 331(6024):1565–1570.
- Pikarsky E, Ben-Neriah Y (2006) NF-kappaB inhibition: A double-edged sword in cancer? *Eur J Cancer* 42(6):779–784.
- Naugler WE, et al. (2007) Gender disparity in liver cancer due to sex differences in MyD88-dependent IL-6 production. *Science* 317(5834):121–124.
- Rakoff-Nahoum S, Medzhitov R (2007) Regulation of spontaneous intestinal tumorigenesis through the adaptor protein MyD88. *Science* 317(5834):124–127.
- Ghiringhelli F, et al. (2009) Activation of the NLRP3 inflammasome in dendritic cells induces IL-1beta-dependent adaptive immunity against tumors. *Nat Med* 15(10):1170–1178.
- Zaidi MR, et al. (2011) Interferon- γ links ultraviolet radiation to melanomagenesis in mice. *Nature* 469(7331):548–553.
- Andreu P, et al. (2010) FcRgamma activation regulates inflammation-associated squamous carcinogenesis. *Cancer Cell* 17(2):121–134.
- de Visser KE, Korets LV, Coussens LM (2005) De novo carcinogenesis promoted by chronic inflammation is B lymphocyte dependent. *Cancer Cell* 7(5):411–423.
- Schwartz-Albiez R, Monteiro RC, Rodriguez M, Binder CJ, Shoenfeld Y (2009) Natural antibodies, intravenous immunoglobulin and their role in autoimmunity, cancer and inflammation. *Clin Exp Immunol* 158(Suppl 1):43–50.
- Bei R, Masuelli L, Palumbo C, Modesti M, Modesti A (2009) A common repertoire of autoantibodies is shared by cancer and autoimmune disease patients: Inflammation in their induction and impact on tumor growth. *Cancer Lett* 281(1):8–23.
- De Palma M, Lewis CE (2013) Macrophage regulation of tumor responses to anti-cancer therapies. *Cancer Cell* 23(3):277–286.
- Solinas G, Germano G, Mantovani A, Allavena P (2009) Tumor-associated macrophages (TAM) as major players of the cancer-related inflammation. *J Leukoc Biol* 86(5):1065–1073.
- Joyce JA, Pollard JW (2009) Microenvironmental regulation of metastasis. *Nat Rev Cancer* 9(4):239–252.
- Kessenbrock K, Plaks V, Werb Z (2010) Matrix metalloproteinases: Regulators of the tumor microenvironment. *Cell* 141(1):52–67.
- Hanahan D, Weinberg RA (2011) Hallmarks of cancer: The next generation. *Cell* 144(5):646–674.
- Hedlund M, Padler-Karavani V, Varki NM, Varki A (2008) Evidence for a human-specific mechanism for diet and antibody-mediated inflammation in carcinoma progression. *Proc Natl Acad Sci USA* 105(48):18936–18941.
- Padler-Karavani V, et al. (2011) Human xeno-autoantibodies against a non-human sialic acid serve as novel serum biomarkers and immunotherapeutics in cancer. *Cancer Res* 71(9):3352–3363.
- Prehn RT (1972) The immune reaction as a stimulator of tumor growth. *Science* 176(4031):170–171.
- Andrews EJ (1971) Evidence of the nonimmune regression of chemically induced papillomas in mouse skin. *J Natl Cancer Inst* 47(3):653–665.
- Prehn RT (2010) The initial immune reaction to a new tumor antigen is always stimulatory and probably necessary for the tumor's growth. *Clin Dev Immunol* 2010: 851728.
- Tangvoranuntakul P, et al. (2003) Human uptake and incorporation of an immunogenic nonhuman dietary sialic acid. *Proc Natl Acad Sci USA* 100(21):12045–12050.
- Calabrese EJ, Blain RB (2011) The hormesis database: The occurrence of hormetic dose responses in the toxicological literature. *Regul Toxicol Pharmacol* 61(1):73–81.
- Crocker PR, Paulson JC, Varki A (2007) Siglecs and their roles in the immune system. *Nat Rev Immunol* 7(4):255–266.
- Varki A, Crocker PR (2009) *Essentials of Glycobiology*, eds Varki A, et al. (Cold Spring Harbor Laboratory Press, Plainview, NY), pp 459–474.
- Soto PC, Stein LL, Hurtado-Ziola N, Hedrick SM, Varki A (2010) Relative over-reactivity of human versus chimpanzee lymphocytes: Implications for the human diseases associated with immune activation. *J Immunol* 184(8):4185–4195.
- Zhang JQ, Biedermann B, Nitschke L, Crocker PR (2004) The murine inhibitory receptor mSiglec-E is expressed broadly on cells of the innate immune system whereas mSiglec-F is restricted to eosinophils. *Eur J Immunol* 34(4):1175–1184.
- McMillan SJ, et al. (2013) Siglec-E is a negative regulator of acute pulmonary neutrophil inflammation and suppresses CD11b β 2-integrin-dependent signaling. *Blood* 121(11):2084–2094.
- Van Rooijen N (1989) The liposome-mediated macrophage 'suicide' technique. *J Immunol Methods* 124(1):1–6.
- Hainsworth JD, et al. (2000) Rituximab monoclonal antibody as initial systemic therapy for patients with low-grade non-Hodgkin lymphoma. *Blood* 95(10):3052–3056.
- Smyth MJ, Hayakawa Y, Takeda K, Yagita H (2002) New aspects of natural-killer-cell surveillance and therapy of cancer. *Nat Rev Cancer* 2(11):850–861.
- Willett WC (2000) Diet and cancer. *Oncologist* 5(5):393–404.
- Larsson SC, Wolk A (2006) Meat consumption and risk of colorectal cancer: A meta-analysis of prospective studies. *Int J Cancer* 119(11):2657–2664.
- Cho E, et al. (2006) Red meat intake and risk of breast cancer among premenopausal women. *Arch Intern Med* 166(20):2253–2259.
- Taylor EF, Burley VJ, Greenwood DC, Cade JE (2007) Meat consumption and risk of breast cancer in the UK Women's Cohort Study. *Br J Cancer* 96(7):1139–1146.
- Linos E, Willett WC, Cho E, Colditz G, Frazier LA (2008) Red meat consumption during adolescence among premenopausal women and risk of breast cancer. *Cancer Epidemiol Biomarkers Prev* 17(8):2146–2151.
- Wallace K, et al. (2009) The association of lifestyle and dietary factors with the risk for serrated polyps of the colorectum. *Cancer Epidemiol Biomarkers Prev* 18(8):2310–2317.
- Lam TK, et al. (2009) Intakes of red meat, processed meat, and meat mutagens increase lung cancer risk. *Cancer Res* 69(3):932–939.
- Tasevska N, et al. (2009) A prospective study of meat, cooking methods, meat mutagens, heme iron, and lung cancer risks. *Am J Clin Nutr* 89(6):1884–1894.
- Sinha R, Cross AJ, Graubard BI, Leitzmann MF, Schatzkin A (2009) Meat intake and mortality: A prospective study of over half a million people. *Arch Intern Med* 169(6): 562–571.
- Ferrucci LM, et al. (2009) Dietary meat intake in relation to colorectal adenoma in asymptomatic women. *Am J Gastroenterol* 104(5):1231–1240.
- Balkwill F, Mantovani A (2001) Inflammation and cancer: Back to Virchow? *Lancet* 357(9255):539–545.
- Seibold HR, Wolf RH (1973) Neoplasms and proliferative lesions in 1065 nonhuman primate necropsies. *Lab Anim Sci* 23(4):533–539.
- Varki NM, Strobert E, Dick EJ, Jr., Benirschke K, Varki A (2011) Biomedical differences between human and nonhuman hominids: Potential roles for uniquely human aspects of sialic acid biology. *Annu Rev Pathol* 6:365–393.

Supporting Information

Pearce et al. 10.1073/pnas.1209067111

SI Methods

Murine Models. *Cmah*^{-/-} mice were generated as previously described (1). *Siglece*-null (*SigE*^{-/-}) mice were generated by McMillan et al. (2). The *Cmah*^{-/-} *SigE*^{-/-} model was generated by breeding *Cmah*^{-/-} and *SigE*^{-/-} mice together, and *Rag1*^{-/-} mice were purchased from the Jackson Laboratory. These mice were bred in C57BL/6 background. Athymic nude mice were bred at the University of California, San Diego on a BALB/c background. All mice were maintained in the University of California, San Diego vivarium according to Institutional Review Board guidelines for the care and use of laboratory animals at University of California, San Diego (Institutional Animal Care and Use Committee).

Generation of Anti-Glycolylneuraminic Acid Antibodies. *Cmah*^{-/-} mice were immunized (via i.p. injection) with 200 μ L of equal-volume erythrocyte membrane ghosts [chimpanzee (*N*-glycolylneuraminic acid [Neu5Gc]-positive) or human (control, Neu5Gc-negative) 200- μ g protein in phosphate-buffered saline (PBS)] and Freund's complete adjuvant. A booster injection using Freund's incomplete adjuvant with the same amount of immunogen was given 2 wk later. An additional booster was given 2 wk after the first booster injection. Two weeks later, serum was collected for analysis of anti-Neu5Gc IgG. Adsorption was performed using 300 μ L of packed washed human RBCs incubated with 2 mL of the isolated sera at 4 °C for 2 h, and the RBCs were subsequently removed by centrifugation. This procedure was repeated five times. Anti-Neu5Gc-positive sera were pooled based on high or low avidity for two to three linked Neu5Gc glycan ELISA targets.

Cell Culture and Preparation of Tumor Cell Lines. MC38 tumor cells were cultured in DMEM high glucose with 10% (vol/vol) FCS, sodium pyruvate, nonessential amino acids, and 1% penicillin streptomycin (all from Gibco Life Technologies). Lewis lung carcinomas (LLC) tumor cells and cell lines made from tumors were cultured in DMEM high glucose with 10% (vol/vol) FCS and 1% penicillin streptomycin. Ramos cells were cultured as per the LLC cells in suspension. MC38 and LLC cells were prepared and administered to mice using the following protocol. Cells were lifted from culture by first washing with PBS and then incubating at room temperature (RT) with 2 mM EDTA in PBS solution. Cells were lifted using a cell scraper. Cells were diluted 1:1 with PBS plus Ca/Mg, pelleted (400 \times g for 5 min), and resuspended in PBS plus Ca/Mg at 4 °C. Cells were counted using a cytometer with trypan blue (Gibco Life Technologies). A note of live vs. dead cells was made. The cell concentration was corrected to 2.5 million live cells per milliliter with PBS plus Ca/Mg. Before inoculation, cell solutions were stored at 4 °C for no longer than 1 h. After inoculation, a sample of the cells was counted with trypan blue and the percentage of live vs. dead cells was compared with the first count. These counts were always comparable within the window of time used (30 min to 2 h).

Flow Cytometric Analysis of Tumor Immune Cell Infiltrates. For analysis of immune cell infiltrates, s.c. tumors were minced with razor blades and digested for 30 min at 37 °C with 1 mg/mL collagenase/dispase (Roche Bioscience). Subsequently, single-cell suspensions were prepared using cell strainers (BD Biosciences). Prepared cell suspensions were incubated with anti-CD45, anti-CD11b, anti-Ly6G, and anti-NK1.1 (all from BD Pharmingen), as well as anti-F4/80 and anti-CD49b (both from

Biolegend). Analysis was performed on a FACSCalibur (BD Biosciences).

Immunohistochemistry of Immune Infiltrates. Cryosections of s.c. tumors were obtained after freezing unfixed tissue in optimal cutting temperature compound (Tissue-Tek; Sakura), and fixation with neutral formaldehyde was performed after blocking endogenous biotin with avidin (Vector). Primary monoclonal antibodies against F4/80 (AbD Serotec); Ly6G, CD3e, and B220 (all from BD Pharmingen, San Diego, CA); and a polyclonal antibody against NKp46 (R&D Systems) were used. Slides were subsequently incubated with corresponding biotinylated secondary antibodies and streptavidin-HRP. Finally, slides were stained with the AEC kit, and nuclei were counterstained with Meyer's hematoxylin (both from Vector).

Flow Cytometry. Analysis of cell surface Neu5Gc expression. Cells were analyzed for Neu5Gc expression according to the manufacturer's protocol (Gc-Free basic kit; Sialix).

Analysis of immunized mouse sera staining to MC38 cells. To periodate or mock-periodate treat cells, cells were incubated with sodium periodate (100 μ L, 2 mM for 10 min at 4 °C) in the dark before staining with the primary antibody. The reaction was quenched with sodium borohydride (20 mM final concentration at RT for 20 min) in the dark. Cells were pelleted (400 \times g for 5 min) and then washed with PBS (1% fish gelatin, 1 mL), repeated several times. To mock-treat, periodate and sodium borohydride were mixed before incubation with cells. Cells were then incubated with the primary sera (chimpanzee or human erythrocyte ghosts) diluted 100-fold (30 min at 4 °C). Secondary Alexa Fluor 647 goat anti-mouse IgG (Invitrogen) was diluted 1,000-fold (30 min at 4 °C).

ELISA for the detection of anti-Neu5Gc IgG from immunized mouse sera. Streptavidin-coated 384-well plates (Pierce) were used. Biotinylated glycans, Gc2-3Lac-Biot and Gc2-6Lac-Biot, were coated in PBS or Tris-buffered saline (TBS) plus 0.5% cold water fish skin gelatin (PBSG/TBSG) at a concentration of 4 ng of glycan per well in 30- μ L volumes. Four wells per sera were to be used (two with periodate treatment and two without). Standards and biotinylated mouse IgG were coated in 1:2 serial dilutions from 80 ng and 10 ng per well in 30- μ L volumes. Wells were coated overnight at 4 °C. Wells were washed three times for 5 min each time with 60 μ L of PBS. Sodium metaperiodate (NaIO₄; 2 mM) was prepared fresh by diluting NaIO₄ (1.37 mg) in 3.2 mL of PBS. NaIO₄ (2 mM) was stored in the dark on ice until use. Sodium borohydride (NaBH₄; 100 mM) was prepared fresh by dissolving NaBH₄ (3.0 mg) in 800 μ L of PBS. NaBH₄ was stored in the dark until use. The total volume prepared was at minimum to minimize leftover borate waste. Wells to be treated with periodate were incubated with 80 μ L of 2 mM NaIO₄. Wells mock-treated with periodate were incubated with 20 μ L of 100 mM NaBH₄ added first, followed by 80 μ L of 2 mM NaIO₄. Plates were incubated at 4 °C for 20 min in the dark. The periodate reaction was quenched using 20 μ L of 100 mM NaBH₄ for 10 min at RT in the dark (not added to the mock-treated wells). The mixture was washed three times with 100 μ L of 50 mM NaCH₃COOH and 100 mM NaCl, and it was then incubated with 60 μ L of PBSG/TBSG for 1 h at RT. Wells were emptied, and sera (diluted 1:200 in 30 μ L of PBSG) were incubated for 2 h at RT. Wells were washed three times with 60 μ L of PBSG and then incubated with goat anti-mouse IgG-alkaline phosphatase (AP) (Jackson ImmunoResearch) and diluted 1:5,000 in PBSG for 30 min at RT. Wells were washed three times with 60 μ L of

PBSG and then developed with 30 μ L of *para*-nitrophenylphosphate, AP substrate, at RT; colorimetric reading (OD) was measured at 405 nm. Among mice administered chimpanzee erythrocyte ghosts, 82% generated a response to Neu5Gc (as determined by comparison with the periodate-treated wells) and 43% were classified as generating high-avidity serum (determined by a response to Gc2-3Lac-Biot and higher avidity for MC38 cells). The total IgG content of the sera was determined using a similar protocol. Here, the sera were used as the target at concentrations of 1:1,000, 1:100, and 1:10. Briefly, sera were diluted in 50 mM sodium carbonate-bicarbonate buffer (pH 9.5) at 4 °C overnight. After washing with TBS (pH 7.5) and blocking with TBS plus Tween 20 (TBST) for 2 h at RT, sera were in-

cubated with alkaline phosphatase-conjugated donkey anti-mouse IgG (Jackson ImmunoResearch Laboratories) diluted in TBST at 1:5,000 at RT for 1.5 h. The IgG was quantitated using a standard curve of normal mouse IgG coated to the wells under the same conditions.

Statistical Analysis. Tumor growth kinetics were analyzed by two-way ANOVA with post hoc multiple comparison analysis, and final tumor masses were analyzed using the Student *t* test compared with the control. Survival curves were used to analyze the appearance of detectable tumor masses and statistically analyzed using the log-rank test. GraphPad Prism software was used for statistical analysis.

1. Hedlund M, et al. (2007) N-glycolylneuraminic acid deficiency in mice: Implications for human biology and evolution. *Mol Cell Biol* 27(12):4340–4346.

2. McMillan SJ, et al. (2013) Siglec-E is a negative regulator of acute pulmonary neutrophil inflammation and suppresses CD11b β 2-integrin-dependent signaling. *Blood* 121(11):2084–2094.

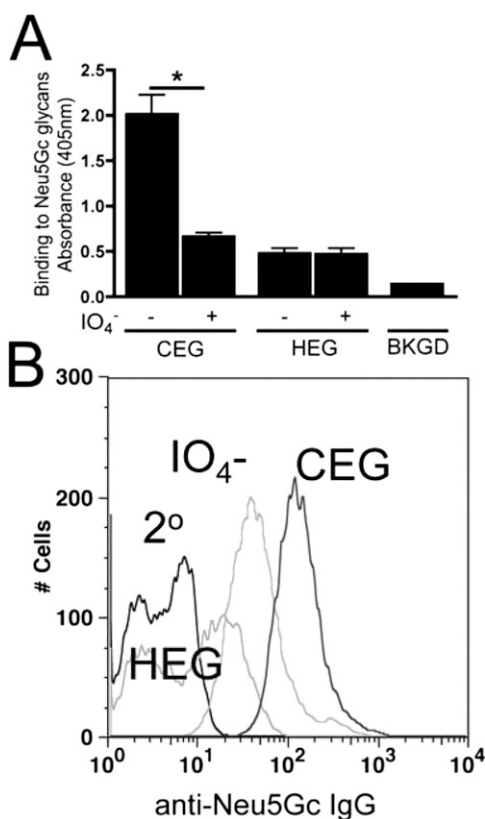


Fig. S1. (A) Syngeneic mouse serum analyzed by ELISA using a Neu5Gc target. CEG, antibodies induced by chimpanzee erythrocyte ghost (anti-Neu5Gc IgG-positive); HEG, antibodies induced by human erythrocyte ghost (control); IO_4^- , mild periodate oxidation. Background (BKGD) served as a PBS control. (B) Flow cytometry analysis of the CEG and HEG serum IgG binding to MC38 cells. $*P < 0.05$.

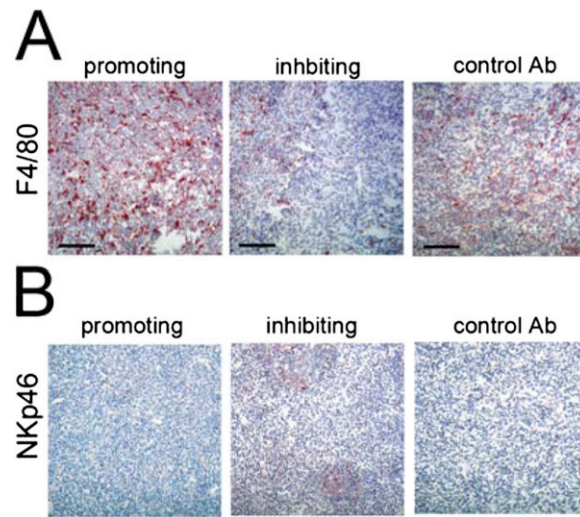


Fig. S3. (A) Tumor tissue taken from promoting (*Left*) or inhibiting (*Center*) dose or control antibody (*Right*) and stained for F4/80⁺ cells. (B) Representative images of natural killer (NK) p46-positive cells infiltrating s.c. MC38 tumors after treatment with a promoting or inhibitory dose or a control antibody dose of antibody-containing sera. For histological analysis, three tumors per condition were studied. (Scale bar, 100 μ m.)

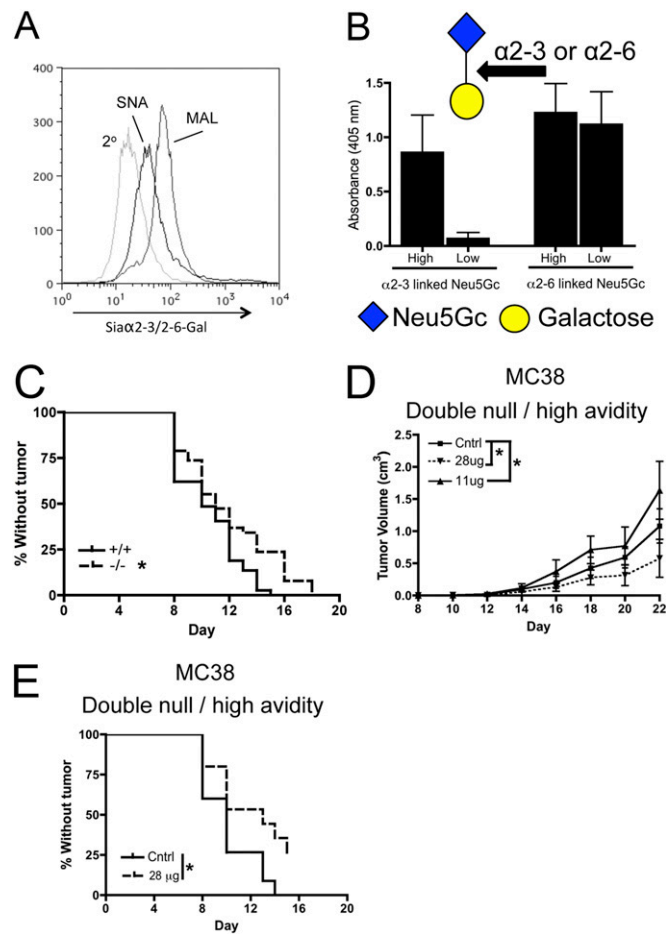


Fig. 54. (A) To help explain the difference in avidity, we probed the surface of the MC38 cell line with two sialic acid (Sia)-binding lectins, *Sambucus nigra* (SNA), which has a preference for Sia α 2-6Gal/GalNAc, and *Maackia amurensis* (MAL), which has a preference for Sia α 2-3Gal β 1-4GlcNAc. Binding of these two lectins is not affected by the types of Sias involved. We found that the MAL bound approximately fivefold higher than the SNA, suggesting α 2-3 Sias are the dominant form on MC38 cells. (B) In keeping with this observation, when analyzing the specificity (ELISA) of the high- vs. low-avidity sera against α 2-3 or α 2-6 linked Neu5Gc targets, only the high-avidity sera contained IgG directed against α 2-3 linked Neu5Gc. (C) Appearance of visible [tumor size defined as >0.2 cm in all three directions measured (length \times width \times depth), giving a minimum volume of 0.008 cm³] tumors in *SigE*^{-/-} (-/-) vs. C57BL/6 WT (+/+) mice. [Data in C are a combination of six comparable experiments (average $n = 6$ per experiment)]. (D) Tumor growth kinetics with anti-Neu5Gc antibodies in a *Cmah*/*Siglec-E* double-null murine model ($n = 7$). (E) Appearance of tumors in *Cmah*^{-/-} *SigE*^{-/-} murine model in the presence of a 28 μ g dose or control antibody. Statistical analysis was performed by two-way ANOVA (C) and a log-rank test (C and E). * $P < 0.05$. Cntrl, control.

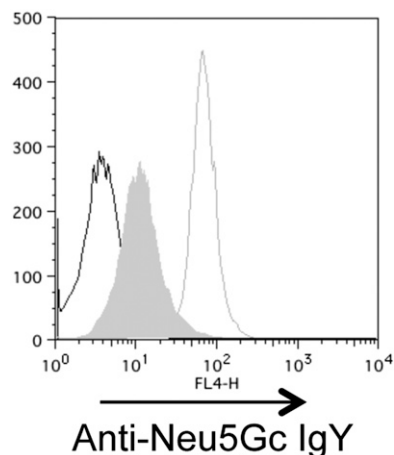


Fig. 55. LLC cells stained with an anti-Neu5Gc IgY (empty gray), oxidized via periodate treatment before IgY staining (solid gray), or isotype control (empty black).

